This is an open access article published under an ACS AuthorChoice License, which permits copying and redistribution of the article or any adaptations for non-commercial purposes.

Langmuir

Article

pubs.acs.org/Langmuir

Controlled Growth of Filamentous Fatty Acid Vesicles under Flow

Christian Hentrich[†,‡] and Jack W. Szostak*[,†,‡,§]

[†]Howard Hughes Medical Institute, Department of Molecular Biology and Center for Computational and Integrative Biology, Massachusetts General Hospital, 185 Cambridge Street, Boston, Massachusetts 02114, United States

[‡]Department of Genetics, Harvard Medical School, 77 Avenue Louis Pasteur, Boston, Massachusetts 02115, United States

[§]Department of Chemistry and Chemical Biology, Harvard University, 12 Oxford St., Cambridge, Massachusetts 02138, United States

S Supporting Information

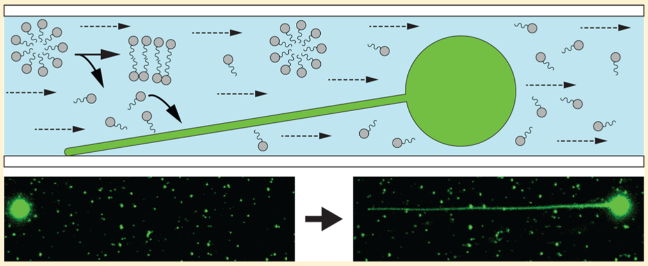

ABSTRACT: The earliest forms of cellular life would have required a membrane compartment capable of growth and division. Fatty acid vesicles are an attractive model of protocell membranes, as they can grow into filamentous vesicles that readily divide while retaining their contents. In order to study vesicle growth, we have developed a method for immobilizing multilamellar fatty acid vesicles on modified glass surfaces and inducing filamentous membrane growth under flow. Filament formation strictly depended on the presence of freshly neutralized fatty acid micelles in the flow chamber. Using light microscopy, we observed a strong dependence of initial growth velocity on initial vesicle size, suggesting that new fatty acid molecules were incorporated into the membrane over the entire external surface of the vesicle. We examined the influences of flow rate, fatty acid concentration, and salt concentration on filamentous growth and observed drastic shape changes, including membrane pearling, of preexisting membrane tubules in response to osmotic stress. These results illustrate the versatility of flow studies for exploring the process of fatty acid vesicle growth following exposure to free fatty acids.

INTRODUCTION

We have been studying a model for the origin of cellular life in which a membranous compartment capable of self-replication encapsulates a functional and genetic biopolymer that is also capable of self-replication.[1] The processes of protocell membrane growth and division are thought to have relied on the self-assembly and self-organization properties of primitive membranes, as it is implausible to assume the existence of complicated cell division machinery at the time of the origin of life.[2,3] Fatty acid membranes are an attractive model for early cell membranes for several reasons beyond their likely prebiotic availability.[4,5] First, fatty acids form membranes spontaneously, given a neutral to slightly basic pH of around 7−8.5 (depending on the length of the aliphatic chain) and a concentration above the critical aggregate concentration.[6,7] A second important aspect is that fatty acid membranes are more permeable than modern diacyl lipid membranes, even allowing for the passive diffusion of charged small molecules like nucleotides across the membrane.[8,9] This high permeability would have been essential in primitive cells prior to the evolution of membrane transport machinery.[10] Another argument for fatty acids as components of early cell membranes is the existence of a simple biochemical pathway leading from fatty acid precursors to phospholipids. Moreover, phospholipids are miscible with fatty acids in membranes, and the presence of phospholipids confers a demonstrable selective growth advantage to membranes of mixed composition.[11,12] Finally, our lab has previously shown that fatty acid vesicles exhibit a peculiar growth behavior: instead of growing spherically in the fashion of an inflating balloon, multilamellar fatty acid vesicles grow through the formation of filamentous membrane tubes.[13] Because this complex self-organized growth is currently not well understood, we set out in this study to examine filamentous growth under controlled conditions.

Whereas phospholipids possess two aliphatic chains and a polar headgroup, fatty acids are composed of only a single aliphatic chain connected to a carboxyl group. This chemical difference leads to several important biophysical differences between fatty acid and phospholipid membranes. Fatty acids are much more water-soluble than phospholipids. While phospholipid vesicles are typically in equilibrium with subnanomolar concentrations of free phospholipid, fatty acids have critical aggregate concentrations of 0.1−100 mM, depending exponentially on chain length.[11,14] The desorption and flip-flop rates of fatty acids are also significantly greater than those of phospholipids, leading to membranes that are much more dynamic than phospholipid membranes, with average residence times of fatty acids in the membrane in the range of milliseconds to seconds.[11,15] Net-neutral phospholipid membranes are relatively robust to changes in pH, whereas fatty acid membranes form over a restricted pH range, when roughly half of the carboxylic acid groups are charged, resulting in

Received: October 6, 2014
Revised: November 14, 2014
Published: November 17, 2014

hydrogen bonds between headgroups.[16] Fatty acid membranes, however, do not form at the pK_a of free carboxylic acids; instead, the pK_a of fatty acids at the membrane surface is shifted upward by about 4 pH units to a pK_a of about 7−8.5, depending on chain length.[14,17] This effect has been explained as the result of a local decrease of pH close to the membrane due to the local enrichment of hydronium cations close to polyanionic surfaces.[18,19] Additionally, hydrogen bonding between protonated and deprotonated carboxylates increases the pK_a of the fatty acids in a membrane context.[20] At low pH fatty acids are fully protonated and form an oil phase, whereas at high pH they are fully deprotonated and form micelles.[21]

Fatty acid vesicles grow when alkaline micelles (the aggregate form of fatty acids at high pH) are added to a buffered solution of lower pH.[22−24] The pH drop causes the micelles to transform into vesicles, and during that transition micelles can also drive the growth of preformed vesicles. This growth-promoting potential declines over time as micelles transform into *de novo* vesicles and lasts for roughly 20 min in the absence of preformed vesicles.[22] When exposed to such a solution, preformed small, unilamellar vesicles (100 nm) grow in two phases: a rapid phase lasting 1−2 s followed by a slow phase lasting roughly 1 min.[22] When observing the growth of larger vesicles in the microscope, an interesting growth mechanism was observed: instead of growing into larger spheres, vesicles grew as filamentous membrane tubes.[12,13] This mode of growth is a consequence of the multilamellarity of the initial vesicles and begins with the formation of a thin unilamellar filamentous protrusion from the outermost bilayer membrane, presumably due to increased lateral pressure within this membrane as it absorbs additional fatty acid monomers. Over time, the filament grows in length, and the contents of the initial vesicle equilibrate throughout the length of the filamentous vesicle. The filamentous shape results from the faster increase of surface area relative to volume, which is osmotically constrained. Eliminating osmotic constraints and therefore also removing the imbalance between surface area and volume growth abolishes filamentous growth.[13] Interestingly, filamentous growth due to a surface area/volume imbalance has also been observed *in vivo* in L-form bacteria, which lack a cell wall.[25]

The membrane tubes that are generated during the growth of large fatty acid vesicles are interesting not only because they illustrate the remarkable self-organizing behavior of small amphiphilic molecules but also because they predispose the vesicle for division by mechanical or photochemical processes.[13,26] This filamentous growth, however, has to date been difficult to observe in detail due to rapid Brownian motion of vesicles during growth. Here, we developed an assay that allows for the immobilization of fatty acid vesicles on the surface of glass slides and thus makes long-term observation of growing vesicles possible. In this configuration, vesicle growth can be observed under constant flow. Furthermore, it is possible to change the outside solution surrounding the vesicles without disrupting the membrane. We report here the use of this assay to study the effects of salt concentration, flow rate and fatty acid concentration on vesicle growth as well as the effects of osmotic stress on filamentous vesicles.

■ EXPERIMENTAL SECTION

Vesicle and Micelles. Fatty acid vesicles were prepared by mixing 10 mM liquid oleic acid (Nu-Check, Elysian, MN), 20 nM biotin-PEG(5K)-DSPE (biotin−poly(ethylene glycol)−distearoylglycerophosphoethanolamine, Nanocs, Boston, MA, 100 μM stock in water), 10 mM HPTS (8-hydroxypyrene-1,3,6-trisulfonate, Sigma-Aldrich, St. Louis, MO, 200 mM stock in water), 5 mM NaOH, and buffer (as described, default is 50 mM bicine (Sigma-Aldrich, St. Louis, MO), 75 mM NaCl, pH 8.5 adjusted with NaOH) and rotating the mixture overnight at room temperature at 6 rpm. Before the experiments, the vesicles were filtered over a short (1 cm) Sepharose 4B (Sigma-Aldrich, St. Louis, MO) size exclusion column and then diluted 1:3 in buffer containing 1 mM unlabeled oleic acid vesicles (containing neither biotinylated lipid nor HPTS) to achieve optimal binding density.

Micelles were prepared by mixing 1 equiv of NaOH with 1 equiv of liquid oleic acid in water and rotating the solution overnight at room temperature (default concentration: 8 mM).

Surface Chemistry. 15 mm round #1 and #1.5 coverslips were purchased from Warner Instruments, Hamden, CT. Surface functionalization was performed by a combination of two previously established protocols.[27,28] Briefly, the coverslips were etched for 30 min with piranha solution (7 parts concentrated H_2SO_4 mixed with 3 parts 30% H_2O_2), washed extensively with water, and then dried using a spin dryer (Technical Video, Woods Hole, MA). The bottom coverslip (#1) was then incubated in 3% (v/v) (trimethoxysilyl)-propylethylenediamine (Sigma-Aldrich, St. Louis, MO) dissolved in 95% methanol/5% acetic acid (v/v) for 60 min. Coverslips were then washed extensively with acetone and again spin dried. Next, coverslips were incubated in a 25% (w/v) solution of PEG (10% Biotin-PEG(3K)-NHS, 90% methoxy-PEG(2K)-NHS, both Rapp Polymere, Tübingen, Germany) in 0.1 M sodium bicarbonate overnight. The following day, the functionalized coverslips were washed extensively with water, spin dried, and stored at 4 °C. The top coverslip (#1.5) was incubated after etching with 10% Cytop-silane in CT solvent 180 (both AGC, Tokyo, Japan) overnight, washed in CT solvent, spin dried, and stored at 4 °C.

Flow Chamber and Setup. Experiments were performed in a custom flow chamber built by Warner Instruments on the basis of their PFC1 flow chamber. The design differs in the use of a #1 15 mm coverslip at the bottom and the possibility to use 100 μm gaskets. The overall flow chamber volume with a 100 μm gasket is 18 μL. The diameter of the flow chamber is 10 mm. Therefore, a flow rate of 1 μL/min at the pump is equivalent to an average flow velocity of 1 mm/min. The flow velocity at the surface where the vesicles are immobilized is lower due to the characteristic velocity distribution of laminar flow. The approximate fluid shear stress at the surface can be calculated as $\tau = 6\mu Q/wh^2$, where μ is the viscosity, Q is the flow rate, w is the chamber width, and h is the chamber height.[29] With an assumed viscosity of 1 cP, the approximate shear stress at our standard flow rate of 20 μL/min is 0.02 Pa (0.2 dyn/cm^2). At the highest flow rates used during growth (100 μL/min), the shear stress is approximately 0.1 Pa (1 dyn/cm^2).

The flow chamber was connected to an electric PC controlled six-channel valve (Idex, Oak Harbor, WA) connected in turn to four manual syringe pumps, a single syringe motorized pump (Kats Scientific, Grand Prairie, TX), and an independently controllable two-syringe motorized pump (Harvard Apparatus, Holliston, MA) that is connected to a static mixing tee (Upchurch Scientific, Oak Harbor, WA). For a typical experiment, the flow chamber was prepared with the following solutions: (1) 200 μL of buffer, (2) 200 μL of 0.05 mg/mL Streptavidin (Sigma-Aldrich, St. Louis, MO) in buffer, incubation for 5 min, (3) 500 μL of buffer with 1 mM oleic acid, incubation for 5 min, (4) 200 μL of labeled, gel-filtered, prediluted vesicles, incubation for 5 min, and (5) 500 μL buffer with 1 mM oleic acid. The experiment was started by flowing through a continuously freshly created mixture of buffer (typically at 18 μL/min) and micelles (typically at 2 μL/min) using the two-channel pump and the mixing tee.

Microscopy and Data Analysis. Images and movies were recorded with a TE-2000 microscope (Nikon, Tokyo, Japan) equipped with a motorized filter turret (Nikon, Japan), standard fluorescence filter cubes (Nikon, Tokyo, Japan), shutters (Sutter, Novato, CA), an EMCCD camera (Andor, Belfast, UK) and using a 20× ELWD

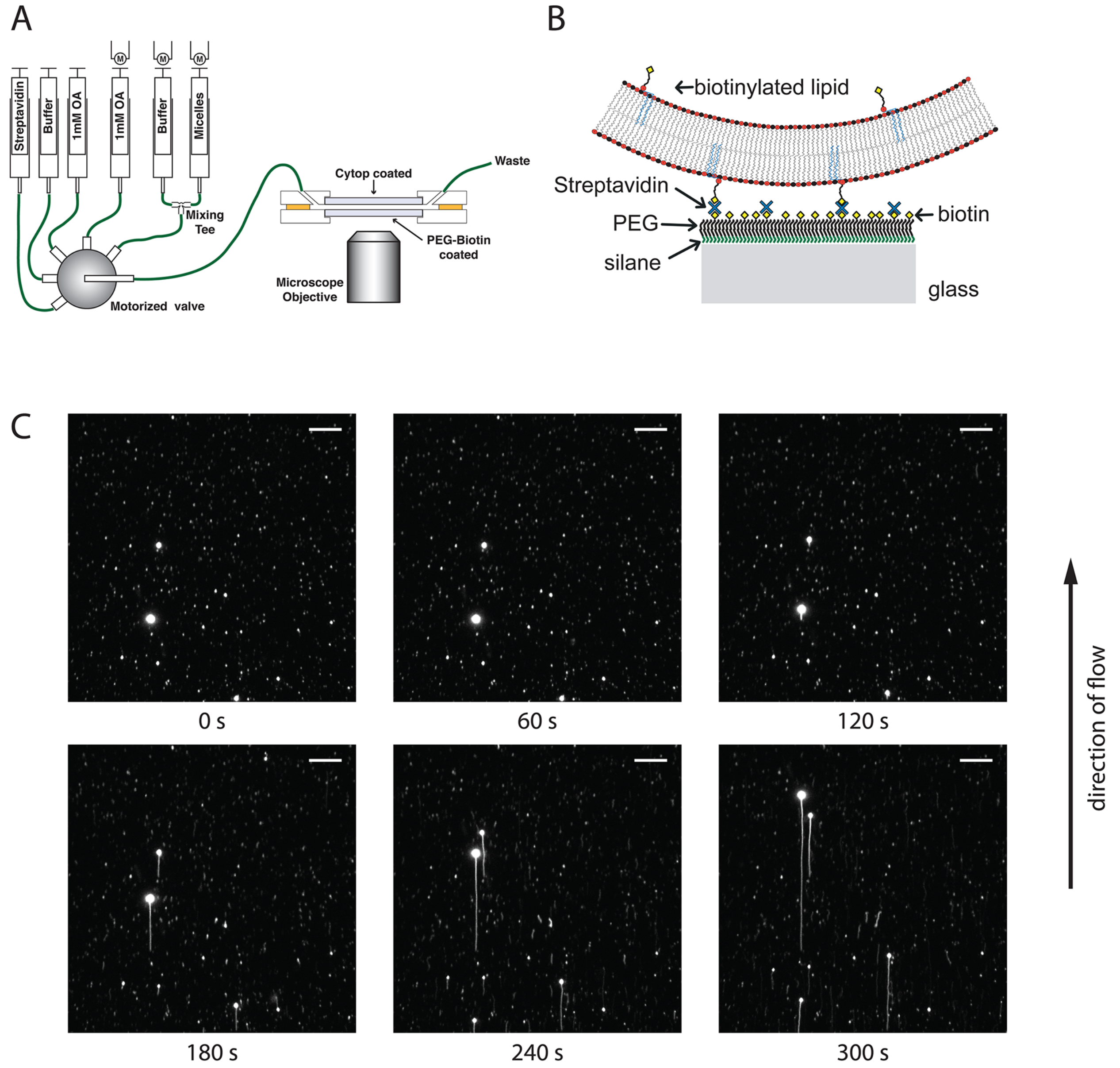

Figure 1. Filamentous growth of immobilized fatty acid vesicles. (A) Scheme of the experimental setup. The flow chamber (above the objective) is connected to a motorized valve, which is connected to several manual syringe pumps, a motorized pump, and a mixing tee, which is in turn connected to a motorized two-channel syringe pump. (B) Scheme of immobilized fatty acid vesicles. The glass surface (gray) is covalently modified with aminosilane (green), to which a dense layer of poly(ethylene glycol) (PEG) is coupled. A fraction of the PEG is modified with biotin (yellow squares). Vesicles consisting of 50% charged (red) and 50% neutral fatty acids also contain a small fraction of Biotin-PEGylated phospholipids (blue/black/yellow). The biotin molecules on the surface are cross-linked to those on the vesicle by tetrameric streptavidin (yellow). (C) Filamentous growth of immobilized vesicles (containing 10 mM HPTS) at 75 mM NaCl, 50 mM Bicine/NaOH pH 8.5, and 0.8 mM oleic acid micelles at a flow rate of 20 μL/min. Flow is already present at t = 0 s, but there is a delay before the growth starts due to the dead volume between valve and flow chamber, which illustrates the immobilization of vesicles (panels 1 and 2). Filamentous growth starts once the buffer/micelle mixture reaches the vesicles (panel 3). Scale bars are 30 μm. The panels are frames of Movie M1.

objective (to achieve a large depth of field). The microscope was controlled by Micro-Manager.[30] Image analysis was performed with using ImageJ.[31] For the determination of growth velocities, kymographs from a representative sample of the growing vesicle population were produced manually, and the rate (inverse slope) was measured by manually approximating a line to the kymograph. At each time point, images were exposed twice: once briefly, with low exposure, to avoid saturation and accurately determine vesicle diameter and once for a longer time to clearly visualize the vesicle thread (typically 20 and 200 ms). Data were analyzed using Excel (Microsoft) and Origin (OriginLab). In box plots, the box limits are the 25th and 75th percentile, and whiskers are outliers within 1.5 interquartile ranges from the box limits. The median is marked by a central line and the mean by an open square. Small crosses mark the 1st and 99th percentile, and small bars mark the maximal/minimal values. Figures were assembled with Illustrator (Adobe).

■ RESULTS

We wished to follow the growth of filamentous membrane tubules following the addition of free fatty acids in an environment that would allow us to control the growth conditions while being compatible with detailed microscopic observations. We therefore set up a flow chamber that would allow for the microscopic observation of immobilized vesicles under continuous flow, with the ability to switch the composition of the solutions flowing over the vesicles. The chamber contained a modified glass surface that allowed for the immobilization of preformed vesicles (Figure 1A). To prepare this surface, we covalently modified the surface of glass coverslips with Biotin-PEG molecules that both contributed to the passivation of the surface and allowed us to use the biotin−streptavidin system for immobilization (Figure 1B). We prepared oleic acid vesicles containing a small percentage (0.0002 mol %) of a biotinylated lipid (DSPE-PEG-Biotin) by overnight tumbling in a buffered solution (see Experimental Section). These vesicles contained the water-soluble fluorescent dye hydroxypyrene trisulfonate (HPTS), which is highly charged and thus cannot diffuse across intact membranes, ensuring that only intact, pre-existing vesicles were visible in the microscope. The function of the biotin was to bind to streptavidin, a homotetrameric protein with four strong biotin binding sites that could act as cross-linker between membrane-bound biotin and glass-surface bound biotin molecules. To immobilize vesicles, we first incubated the flow chamber with streptavidin, washed out unbound streptavidin, and then flowed the HPTS/biotin labeled vesicles into the flow chamber. After another wash to remove unbound vesicles, we observed the stable immobilization of the remaining vesicles on the surface using fluorescence microscopy (Figure 1C, panels 1 and 2; Movie M1, first minute). Similar immobilization techniques have been used in the past to immobilize phospholipid vesicles or cytoskeletal filaments.[32,33]

We then examined the behavior of immobilized vesicles when exposed to a continuous flow of the growth-promoting micelle solution. Because the alkaline micelle solution must be neutralized to avoid dissolving the immobilized vesicles and to allow growth to occur, we flowed a solution of freshly neutralized oleate micelles (which are thus in the process of transforming into vesicles) through the flow chamber. These freshly neutralized micelles were prepared by continuous mixing of alkaline micelles with buffer just before entering the flow chamber. In this way the concentration and growth-promoting potential of the freshly neutralized micelles are kept constant over time, as freshly mixed solution passes over the surface of immobilized vesicles at a constant flow rate. Based on a typical flow rate of 20 μL/min and the 60 μL dead volume of the system, the oleate micelles would reach the immobilized vesicles approximately 3 min after neutralization. Under these conditions, we observed that most vesicles exhibited filamentous growth that could be sustained for long periods of time, e.g. 30 min or more, resulting in filament lengths of 500 μm or longer. The newly generated filaments extended from the initial point of attachment to the biotinylated surface, to the parental spherical vesicle which was carried downstream by the flowing fluid. It was easy to observe and measure growth since the filaments were aligned by the flow (Figure 1C and Movie M1). In previous experiments done in the absence of flow it was unclear how many filaments could grow per vesicle,[13] while with flow almost all vesicles we observed (>99%) had only a single filament connecting the point of surface attachment to the spherical vesicle.

Vesicles prepared by lipid hydration are multilamellar and very heterogeneous in size, ranging at least from 0.1 to 10 μm in diameter.[21] We used this property to test whether the growth rate depended on vesicle size. For example, in a simple scenario, in which free fatty acid uptake occurs over the surface, and in which filamentous protrusions initiate as unilamellar structures of the same diameter, one would expect the initial growth rate to depend on the vesicle surface area. To test this idea, we measured initial vesicle sizes and initial growth velocities (i.e., change in filament length vs time) for vesicles growing in 0.8 mM oleic acid micelles, freshly neutralized in 50 mM Na^+-bicine pH 8.5, 75 mM NaCl at a flow rate of 20 μL/min.

We observed that the initial growth velocity does indeed depend on the initial size of the vesicle, although with a large degree of inherent noise (Figure 2A and Figure S1). Furthermore, many small vesicles (but also some large ones) did not grow filaments during the course of the experiments. This variability might be a consequence of the large variability of the polydisperse vesicles in lamellarity and/or internal structure.[14,34] In velocity measurements derived from kymograph analysis, we measured the initial velocity over the first 60 s of filament growth, during which the increase in filament length was nearly linear with time. It is clear that on average filaments extending from larger vesicles elongated more rapidly than filaments extending from smaller vesicles. However, because of the high degree of variability, it was not possible to distinguish between a growth rate proportional to the square of vesicle diameter, as expected from the incorporation of new fatty acids throughout the vesicle surface (along with constant filament diameter), vs growth linearly proportional to vesicle diameter, as expected from incorporation of new fatty acids over the entire surface, but with filament diameter proportional to initial vesicle diameter. In many instances, we observed an acceleration of growth velocity at late times in the experiment

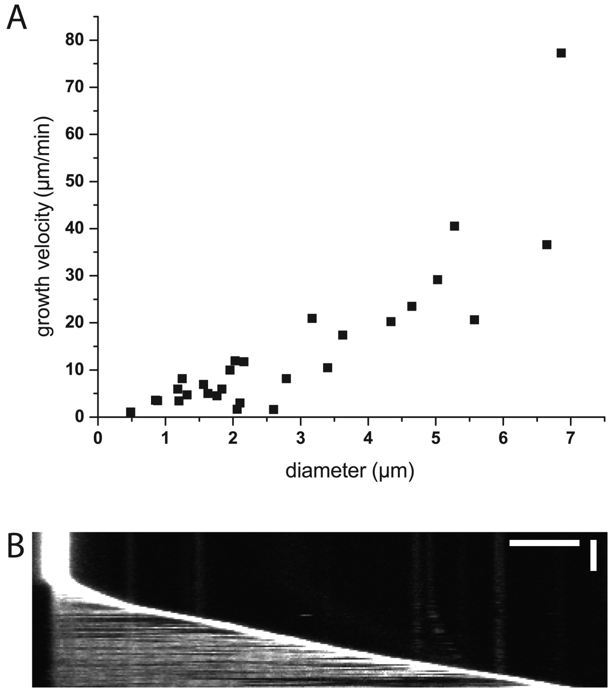

Figure 2. Size dependence of vesicle growth velocity. (A) Vesicle size correlates with tubule growth velocity. Initial filament growth velocities (as measured by kymograph analysis) of vesicles at 75 mM NaCl, 50 mM Bicine pH 8.5 (with NaOH), and 0.8 mM oleic acid micelles with a flow rate of 20 μL/min are plotted against vesicle diameter. (B) Kymograph (time−space plot) of a growing vesicle (from Figure 1). The slope is becoming steeper over time, indicating an acceleration of growth. Scale bars: 20 μm (horizontal); 60 s (vertical).

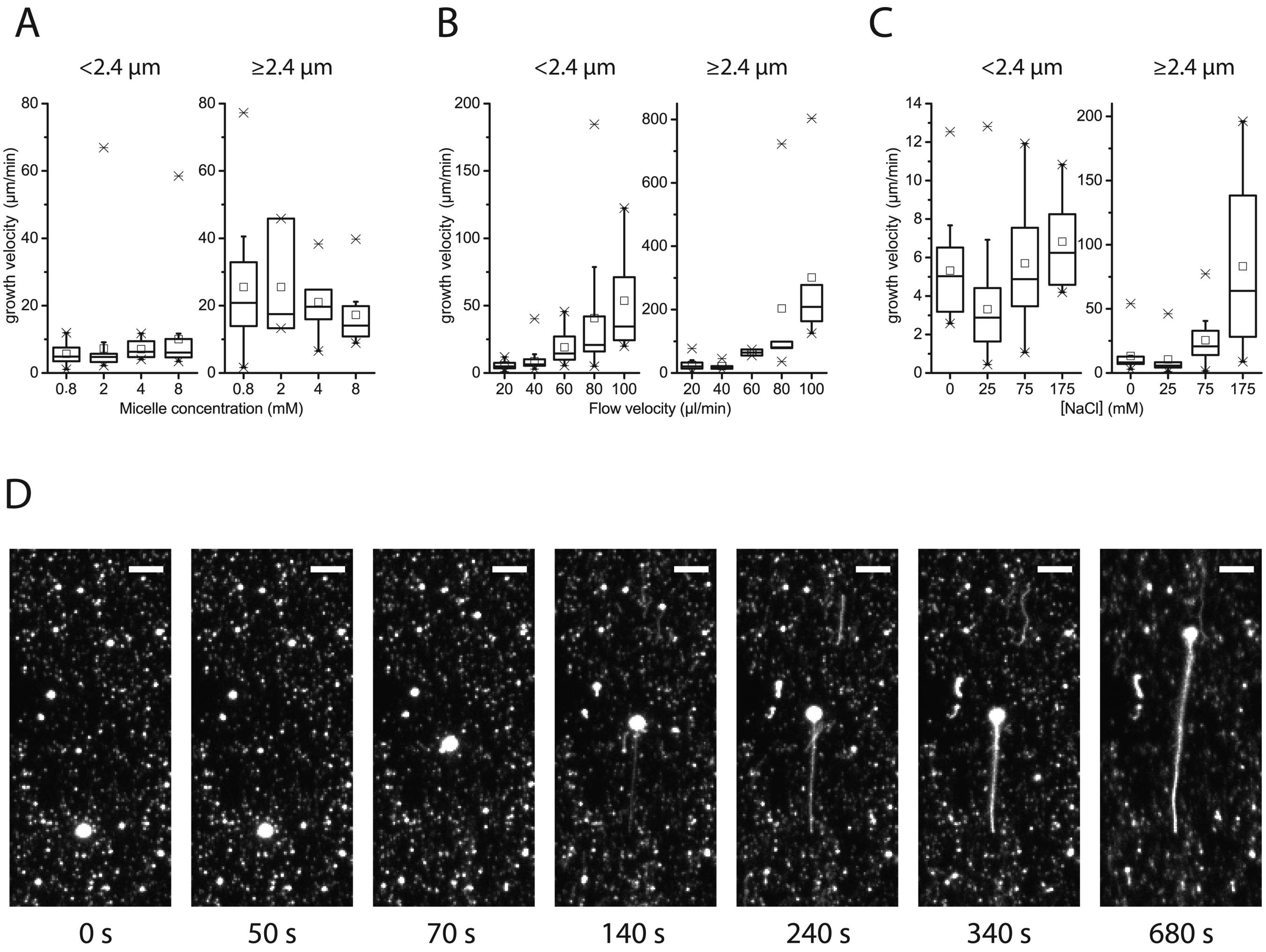

Figure 3. Impact of different conditions on vesicle growth velocity. (A) Box plots of the growth velocity of small (left, diameter below 2.4 μm) and large vesicles (right, diameter above 2.4 μm) at different concentrations of feeding micelles. (B) Box plots of the growth velocity of small and large vesicles at different flow rates. (C) Box plots of the growth velocity of small and large vesicles at different concentrations of sodium chloride. Our standard condition (0.8 mM micelles, 75 mM NaCl, 20 μL/min flow rate) is identical in all three sets of graphs and plotted as a reference. Source data are presented in Figure S1 (see Experimental Section for details on box plots). (D) At high flow rates (here: 100 μL/min), the vesicles are initially rapidly stretched, and then growth stalls until the filament becomes visible. Then the tubule growth continues. Note that the initial stretching is dependent not on the flow rate, but on the presence of the growth solution, as there is no stretching in the first minute (first two panels). Panels are excerpts from Movie M2. Scale bars are 10 μm.

(Figure 2B). The acceleration in growth velocity supports the argument for a dependence of growth velocity on the overall area of the membrane and suggests that fatty acids are incorporated into the filament surface as well as the original vesicle surface (see Figure S2A for additional examples).

To test whether the availability of fatty acids was rate-limiting for filamentous vesicle growth, we varied the concentration of micelles in the freshly mixed growth solution. In order to have a semiquantitative measure for comparing different experimental conditions, we binned the vesicles into small (<2.4 μm) and larger vesicles (≥2.4 μm) and calculated the average growth velocity for each. We observed that varying the concentration of free micelles between 0.8 mM (roughly 8-fold the critical aggregate concentration at pH 8.5) and 8 mM did not significantly influence the filament growth velocity (Figure 3A). This is in accordance with previous measurements of small (100 nm) vesicles in bulk solution[22] and suggests that over this concentration range fatty acids in micelle form are not rate-limiting for vesicle growth.

The flow of buffer alone does not cause the appearance of filaments, and their formation and growth depend strictly on the arrival of freshly mixed micelle/buffer solution in the flow chamber. Prior to the arrival of the micelle/buffer solution, the immobilized vesicles are exposed for ∼3 min to fluid flow in buffer containing unlabeled vesicles (1 mM oleate) to maintain the concentration of free fatty acid at the critical aggregate concentration. No filaments appear during this phase of the experiment, which is due to a dead volume of ∼60 μL and a flow rate of 20 μL/min; part of this period is visible in Movies M1−M4. Our experiments are therefore fundamentally different from the pulling of membrane tubules from vesicles by pipet aspiration, molecular motors, or viscous drag forces.[29,35−38] Having ruled out flow as the underlying cause for membrane tubule formation, we were nevertheless curious to see if varying the flow rate would affect the growth process. For example, stretching of the filaments by viscous drag could alter the apparent growth rate; alternatively, the on-rate of fatty acids onto the filaments could vary with membrane tension. When we varied the flow rate from 20 μL/min (our standard

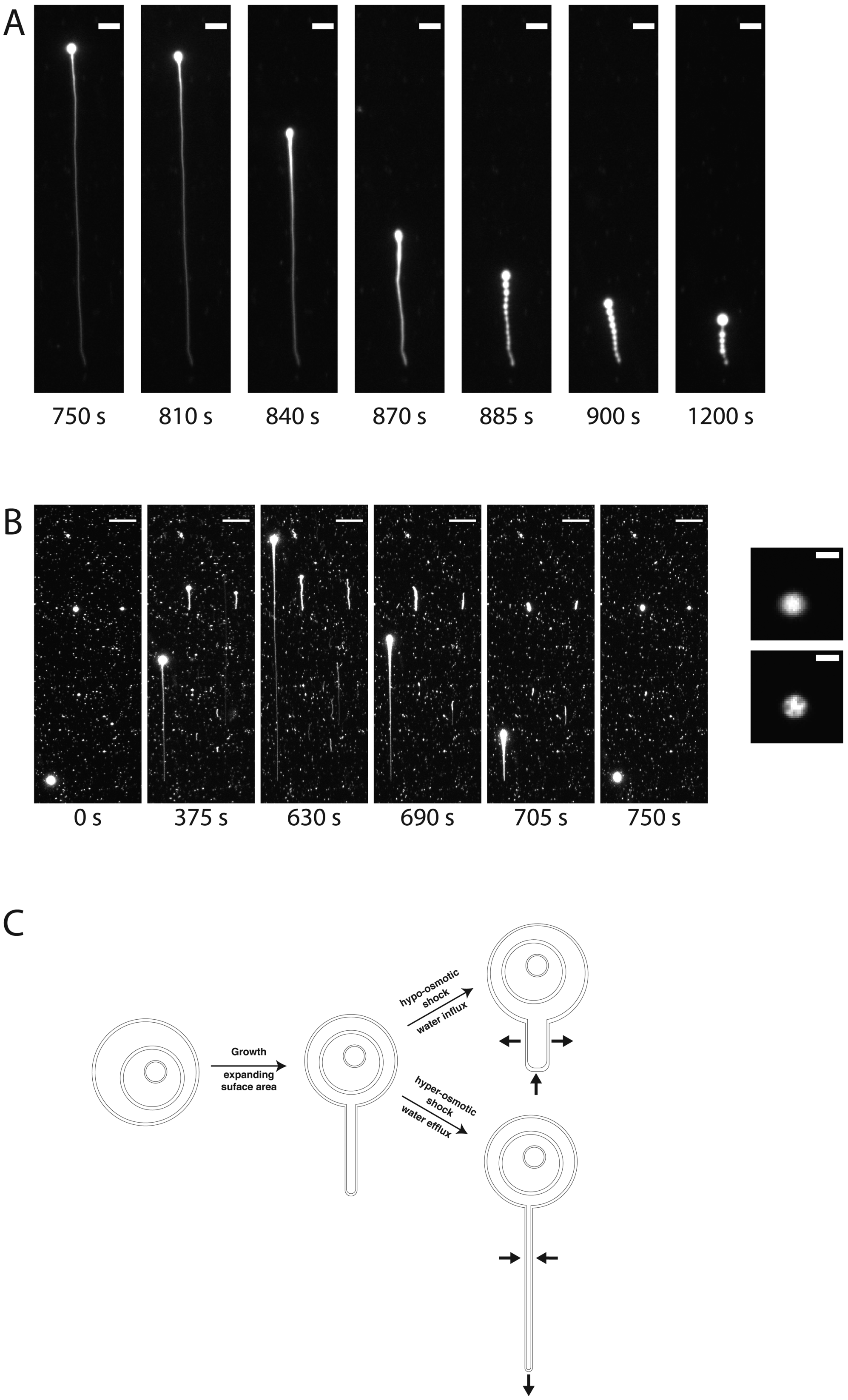
A
750 s
810 s
840 s
870 s
885 s
900 s
1200 s
B
0 s
375 s
630 s
690 s
705 s
750 s
C
Growth
expanding
suface area
hypo-osmotic
shock
water influx
hyper-osmotic
shock
water efflux

Figure 4. Effect of osmotic stress on filamentous vesicles. (A) Lowering the external salt concentration (75 mM NaCl to 25 mM NaCl) leads to an influx of water into the tubule, which therefore contracts, causing pearling. Panels are from Movie M3. For better visibility of the filament, a nonlinear contrast adjustment (gamma value 0.6) was applied to these images. Scale bars are 10 μm. (B) Increasing the external salt concentration (75 mM NaCl to 175 mM NaCl) leads to an efflux of water from the tubule. This causes a rapid elongation in long filaments and an increase in width in shorter filaments (under loss of the spherical vesicle part) (panel 3). This state is however unstable and leads to rapid collapse of the filaments (panels 4–6). Panels are from Movie M4; scale bars are 30 μm. Inset, right: the large vesicle pregrowth and postcollapse at nonsaturating imaging conditions. At the beginning of the experiment, the vesicle has homogeneous fluorescence; after the collapse internal structures are discernible. The

Figure 4. continued

overall fluorescence intensity changed only slightly (2115 ± 7 AU to 1928 ± 7 AU, background corrected measurement over five frames). Scale bars are 5 μm. (C) Scheme of the effect of surface area change (first step) and volume change (second step) on fatty acid vesicles.

condition) to 60 μL/min, we observed an increase in average growth velocity of roughly 3-fold, which could be due to either of the above mechanisms. However, when we further increased the flow rate to 80 or 100 μL/min, we observed a qualitative change in the growth process (Figure 3B). At these high flow rates a thin tube formed very rapidly, then growth stalled as the tube slowly filled with the soluble dye, and then growth continued (Figure 3D and Movie M2). We interpret this as the rapid formation of a very thin membrane tubule whose growth was initially accelerated by viscous drag as the spherical initial vesicle was swept downstream; this rapid growth phase may be analogous to the formation of thin tubules by micropipet aspiration. However, even under these high flow rates, the formation of the tubule depended on the presence of freshly neutralized micelles, as there is no growth observed in the initial 50 s, followed by very rapid growth in the following 10 s (Figure 3D and Movie M2). Thus, the growing filament may be more sensitive to shear forces than the spherical vesicles.[29] The thin filament then slowly expanded in diameter as vesicle contents diffused into the tubule and then filament growth continued. At extremely high flow rates exceeding 500 μL/min, we observed the detachment of filamentous vesicles from the surface, probably reflecting tearing of the membrane (Movie M5).

Next we investigated the effect of the concentration and identity of the fatty acid counterion—factors that directly affect the dynamics of fatty acids and therefore of membrane growth. In the presence of sodium ions, fatty acid membrane growth is accompanied by the stoichiometric flip-flop of fatty acids both in the neutral protonated state and in the form of the sodium salt, so that the inner leaflet of the membrane can grow in concert with the outer leaflet.[39] First we asked whether the concentration of sodium ions in solution would influence tubule growth velocity by affecting either the flip-flop rate or the osmotic balance during vesicle growth. We varied the sodium chloride concentration in the buffer (50 mM Na^+-bicine pH 8.5) from 0 to 175 mM NaCl. We found that increasing the sodium chloride concentration accelerated the size-normalized growth velocity, modestly in small vesicles but by a factor of 3 in larger vesicles (Figure 3C). To differentiate between charge and osmotic effects, we also tested the growth velocity of vesicles prepared and observed in buffers consisting of 50 mM Na^+-bicine (pH 8.5) with 350 mM sucrose or 50 mM bicine + 175 mM arginine + 25 mM NaCl adjusted to pH 8.5 with HCl. We observed negligible growth in sucrose, whereas vesicles in arginine grew very slowly at rates of 1.3/3.3 μm/min (small or large vesicles, respectively) compared to 5.7/25.5 μm/min in our standard conditions with no added salt or osmolyte. As increasing osmolarity by itself did not lead to the same acceleration of growth as observed with sodium chloride, we suggest that the increased growth rate may reflect an increased concentration of sodium oleate in the outer leaflet, leading to faster inward flipping of sodium oleate complexes and thus faster overall membrane growth. The larger increase of growth rate for larger vesicles may be indicative of a relatively larger volume between the two outermost membrane layers in larger vesicles (with regards to surface area), allowing relatively more sodium oleate adducts to flip-flop into larger vesicles than into smaller vesicles.

In addition to studying the effects of environmental conditions on the growth of filamentous vesicles, our flow system can be used to examine the effects of changing conditions on preformed filamentous vesicles. We hypothesized that changes in salt or osmolyte concentration should have strong effects on existing filamentous vesicles due to the semipermeable nature of fatty acid membranes. To test this, we grew oleic acid vesicles into filaments and then switched the flow solution from freshly neutralized micelles to a solution containing unlabeled vesicles (at 1 mM oleate, to maintain free oleate at the critical aggregate concentration) and varying concentrations of salt. When we switched the flow solution to iso-osmotic vesicles, the preformed filaments stopped growing, and slowly shortened over a period of roughly 30 min, possibly due to a slow loss of fatty acid from the filament to the flow solution. In contrast, when we changed the flow solution to a hypo-osmotic vesicle solution, we observed a rapid and simultaneous shortening and widening of the membranous tubules (Figure 4A). During this shape transition, we observed the transformation of the initially smooth filament to a connected string of small spherical vesicles (Figure 4A and Movie M3). This phenomenon has been termed "pearling" and was originally observed when filamentous vesicles were subject to stretching forces.[40] The size of the "pearls" formed in our experiments varied between trials and conditions, but they appeared in every experiment of this kind ($n > 10$). Interestingly, this process could be repeated several times by changing between buffer and micelle solutions, with the second growth rate being faster than the initial rate (Movie M3 and Figure S2B). The initial rapid shortening and thickening of the filament is consistent with a rapid influx of water into the vesicle, causing a decrease in the surface to volume ratio and thus the formation of a shorter, wider tubule (see scheme Figure 4C). The resulting induced membrane tension could then initiate the pearling instability, as previously seen.[40,41]

When we performed the converse experiment of transferring preformed filamentous vesicles into a flow solution of 1 mM oleate vesicles with a higher salt concentration, we observed an initial rapid extension of the tubule. This is consistent with water exiting from the interior of the tubular vesicle, leading to an increase in the surface to volume ratio and hence the formation of a longer, thinner tubule (see Figure 4C). However, these extended tubules were unstable and rapidly collapsed into a spherical vesicle (Figure 4B and Movie M4). The internal structure of the vesicles changed during this process with almost no loss of content, suggesting membrane invagination during the contraction and the formation of compound vesicles (Figure 4B, inset).

■ DISCUSSION

The growth of initially spherical fatty acid vesicles into greatly elongated but still closed filamentous structures is a compelling property that makes these vesicles an attractive system for model protocell membranes because of the ease of division of filamentous vesicles into smaller daughter vesicles.[13] A detailed understanding of the growth and general properties of filamentous vesicles would therefore be helpful in understanding the conditions under which fatty acid-based protocells could grow and divide. We have presented a novel approach that allows for the observation of filamentous growth under defined conditions of continuous flow as well as the observation of changes in filamentous vesicle morphology in response to changes in environmental conditions. Because growing filaments are aligned by flow, our system greatly simplifies the measurement of membrane tubule length vs time. We used this filament length assay to measure the influence of flow rate, micelle concentration, and salt concentration on the rate of filamentous vesicle growth and identified a strong contribution of initial vesicle size to growth velocity.

When fatty acid micelles are shifted from a high pH, at which they are the stable aggregate form, to a lower pH, at which bilayer membranes are the stable phase, they transform into vesicles over a period of minutes.[22] At early stages in this transformation, pH-neutralized micelles can also drive the growth of pre-existing vesicles. The mechanism of this effect remains unclear, but it seems likely that following the pH drop either the micelles themselves (or possibly sheetlike intermediates) are in a transient high-energy state. In this state fatty acid monomers may exist in solution at a concentration exceeding the critical aggregate concentration, thereby driving the growth of pre-existing membranes. Alternatively, the high-energy state of the micelles or sheetlike intermediates may lead directly to membrane growth by a process akin to membrane fusion.[22] Previous experiments have shown that fatty acid monomers can rapidly form micelles whereas formation of vesicles is much slower.[42] Our finding that the concentration of freshly neutralized micelles in the flow solution did not influence the growth velocity significantly suggests that monomer insertion is the rate-limiting step for vesicle growth, assuming that the monomer concentration above the critical aggregate concentration remains approximately constant. The direct addition of fatty acid aggregates to vesicles is less likely because the concentration of such intermediates should linearly increase with the total concentration of fatty acids in the system, and one therefore should observe faster growth at higher micelle concentrations. The observed acceleration of vesicle growth velocity over time suggested that new fatty acid monomers were incorporated not only into the spherical vesicle surface but also into the growing filament. We were not able to detect an initial rapid growth phase as previously observed by stopped flow fluorescence measurements.[22] This might be due to the fact that the growth promoting potential of the freshly neutralized micelles is kept constant due to flow and that there is a delay of approximately 3 min between neutralization and the arrival of freshly neutralized micelles in the flow chamber.

Our observations are consistent with filamentous growth resulting from an imbalance between surface area growth and volume growth due to osmotic constraint[13] (see also Figure 4C). This especially held true for the change of osmotic pressure experiments, where changes of osmotic constraints and therefore volume immediately affected tubule length. Despite reacting to osmotic shifts with dramatic shape changes, filamentous fatty acid vesicles were remarkably resistant to osmotic stress and did not leak contents during these shape rearrangements (Figure 4B, inset). In the context of the origin of life, this is an important quality for a scenario where protocells were exposed to cycles of concentration by evaporation and dilution due to rain.

Previously our lab has shown that filamentous vesicles can divide spontaneously by agitation of the liquid surface.[13] In light of this, it is noteworthy that in the flow chamber system the membrane tubes were difficult to fragment by tearing and very high flow rates were necessary to achieve fragmentation (Movie M5). Membrane fission thus can be difficult even for fatty acid membranes, which makes research into prebiotic abscission mechanisms highly relevant.[43] Our lab has previously demonstrated the possibility of photochemically induced membrane fission,[26] whereas research in L-form bacteria has directly highlighted the importance of membrane fluidity for abscission in the absence of a protein-based cell division machinery.[44]

The assay we developed here has the potential to be useful in many other scenarios for the study of vesicles and model protocells. Recently our lab reported the use of a dialysis device to feed nutrients to model protocells in intervals.[45] In the flow chamber system, such a device would be unnecessary as nutrients can be flowed directly over the vesicles, providing a continuous source of fresh molecules. The immobilization of vesicles also enables long-term observation of individual protocells. Paired with a fluorescent readout of RNA replication,[46] membrane growth and genome replication could be observed simultaneously in individual vesicles.

Finally, it is truly remarkable that all the complex behavior described in this paper stems from the interaction of a very simple chemical, a fatty acid, with its aqueous environment. This extraordinary self-organization behavior of fatty acids[47] is a strong paradigm for how complexity could have emerged spontaneously at the origin of life.

■ CONCLUSION

Fatty acid vesicles are important models of protocell membranes in origin of life research and characteristically exhibit very dynamic behavior. In order to study one such dynamic behavior, namely the growth of spherical fatty acid vesicles into long filaments, we immobilized vesicles on a glass surface and observed them during exposure to fluid flow. Using fluorescence video microscopy, we could measure the rate of growth of the membrane tubules that form when a vesicle comes into contact with freshly neutralized alkaline micelles. We used this assay to study the impact of different environmental conditions on the tubule growth process. We were also able to observe the drastic effects of changes in the external conditions on tubular fatty acid vesicles, including strong but reversible pearling effects. We expect the experimental approach established here to be useful for the study of more complex protocell models as well as further research into fundamental membrane biophysics.

■ ASSOCIATED CONTENT

Ⓢ Supporting Information

Figures S1 and S2; Movies M1−M5. This material is available free of charge via the Internet at http://pubs.acs.org.

■ AUTHOR INFORMATION

Corresponding Author

*Tel 617-726-5981; Fax 617-726-6893; e-mail szostak@molbio.mgh.harvard.edu (J.W.S.).

Notes

The authors declare no competing financial interest.

■ ACKNOWLEDGMENTS

We thank Brian Lee and Lakshminarayanan Mahadevan for helpful discussions. We also thank Aaron Engelhart, Aaron Larsen, Anders Björkbom, Neha Kamat, Noam Prywes, Tony Z. Jia, and Victor Lelyveld for critical reading of the manuscript. J.W.S. is an investigator of the Howard Hughes Medical Institute. This research was supported in part by Grant EXB02-0031-0018 from the NASA Exobiology Program to J.W.S.

■ REFERENCES

(1) Szostak, J. W.; Bartel, D. P.; Luisi, P. L. Synthesizing life. *Nature* **2001**, *409*, 387−90.

(2) Budin, I.; Szostak, J. W. Expanding roles for diverse physical phenomena during the origin of life. *Annu. Rev. Biophys.* **2010**, *39*, 245−63.

(3) Monnard, P. A.; Deamer, D. W. Membrane self-assembly processes: steps toward the first cellular life. *Anat. Rec.* **2002**, *268* (3), 196−207.

(4) McCollom, T. M.; Ritter, G.; Simoneit, B. R. Lipid synthesis under hydrothermal conditions by Fischer-Tropsch-type reactions. *Origins Life Evol. Biospheres* **1999**, *29* (2), 153−66.

(5) Allen, W. V.; Ponnamperuma, C. A possible prebiotic synthesis of monocarboxylic acids. *Curr. Mod. Biol.* **1967**, *1* (1), 24−8.

(6) Gebicki, J. M.; Hicks, M. Ufasomes are stable particles surrounded by unsaturated fatty acid membranes. *Nature* **1973**, *243* (5404), 232−4.

(7) Hargreaves, W. R.; Deamer, D. W. Liposomes from ionic, single-chain amphiphiles. *Biochemistry* **1978**, *17* (18), 3759−68.

(8) Mansy, S. S.; Schrum, J. P.; Krishnamurthy, M.; Tobé, S.; Treco, D. A.; Szostak, J. W. Template-directed synthesis of a genetic polymer in a model protocell. *Nature* **2008**, *454*, 122−5.

(9) Walde, P.; Goto, A.; Monnard, P.-A.; Wessicken, M.; Luisi, P. L. Oparin's reactions revisited: Enzymic synthesis of poly(adenylic acid) in micelles and self-reproducing vesicles. *J. Am. Chem. Soc.* **1994**, *116* (17), 7541−7547.

(10) Mansy, S. S. Membrane transport in primitive cells. *Cold Spring Harbor Perspect. Biol.* **2010**, *2* (8), a002188.

(11) Budin, I.; Szostak, J. W. Physical effects underlying the transition from primitive to modern cell membranes. *Proc. Natl. Acad. Sci. U. S. A.* **2011**, *108* (13), 5249−54.

(12) Peterlin, P.; Arrigler, V.; Kogej, K.; Svetina, S.; Walde, P. Growth and shape transformations of giant phospholipid vesicles upon interaction with an aqueous oleic acid suspension. *Chem. Phys. Lipids* **2009**, *159* (2), 67−76.

(13) Zhu, T. F.; Szostak, J. W. Coupled growth and division of model protocell membranes. *J. Am. Chem. Soc.* **2009**, *131*, 5705−13.

(14) Morigaki, K.; Walde, P. Fatty acid vesicles. *Curr. Opin. Colloid Interface Sci.* **2007**, *12* (2), 75−80.

(15) Simard, J. R.; Pillai, B. K.; Hamilton, J. A. Fatty acid flip-flop in a model membrane is faster than desorption into the aqueous phase. *Biochemistry* **2008**, *47* (35), 9081−9.

(16) Smith, R.; Tanford, C. Hydrophobicity of long chain n-alkyl carboxylic acids, as measured by their distribution between heptane and aqueous solutions. *Proc. Natl. Acad. Sci. U. S. A.* **1973**, *70* (2), 289−93.

(17) Gomez-Fernandez, J. C.; Villalain, J. The use of FT-IR for quantitative studies of the apparent pKa of lipid carboxyl groups and the dehydration degree of the phosphate group of phospholipids. *Chem. Phys. Lipids* **1998**, *96* (1−2), 41−52.

(18) Haines, T. H. Anionic lipid headgroups as a proton-conducting pathway along the surface of membranes: a hypothesis. *Proc. Natl. Acad. Sci. U. S. A.* **1983**, *80* (1), 160−4.

(19) Gouy, M. Sur la constitution de la charge électrique à la surface d'un électrolyte. *J. Phys. Theor. Appl.* **1910**, *9* (1), 457−468.

(20) Kanicky, J. R.; Shah, D. O. Effect of premicellar aggregation on the pKa of fatty acid soap solutions. *Langmuir* **2003**, *19* (6), 2034−2038.

(21) Walde, P.; Namani, T.; Morigaki, K.; Hauser, H. Formation and Properties of Fatty Acid Vesicles (Liposomes). In *Liposome Technology*, 3rd ed.; Informa Healthcare: New York, 2006; Vol. *1*, pp 1−19.

(22) Chen, I. A.; Szostak, J. W. A kinetic study of the growth of fatty acid vesicles. *Biophys. J.* **2004**, *87*, 988−98.

(23) Rasi, S.; Mavelli, F.; Luisi, P. L. Cooperative micelle binding and matrix effect in oleate vesicle formation. *J. Phys. Chem. B* **2003**, *107* (50), 14068−14076.

(24) Blöchliger, E.; Blocher, M.; Walde, P.; Luisi, P. L. Matrix effect in the size distribution of fatty acid vesicles. *J. Phys. Chem. B* **1998**, *102* (50), 10383−10390.

(25) Mercier, R.; Kawai, Y.; Errington, J. Excess membrane synthesis drives a primitive mode of cell proliferation. *Cell* **2013**, *152* (5), 997−1007.

(26) Zhu, T. F.; Adamala, K.; Zhang, N.; Szostak, J. W. Photochemically driven redox chemistry induces protocell membrane pearling and division. *Proc. Natl. Acad. Sci. U. S. A.* **2012**, *109* (25), 9828−32.

(27) Bieling, P.; Telley, I. A.; Hentrich, C.; Piehler, J.; Surrey, T. Fluorescence microscopy assays on chemically functionalized surfaces for quantitative imaging of microtubule, motor, and +TIP dynamics. *Methods Cell Biol.* **2010**, *95*, 555−80.

(28) Rasnik, I.; Myong, S.; Cheng, W.; Lohman, T. M.; Ha, T. DNA-binding orientation and domain conformation of the E. coli rep helicase monomer bound to a partial duplex junction: single-molecule studies of fluorescently labeled enzymes. *J. Mol. Biol.* **2004**, *336* (2), 395−408.

(29) Hochmuth, R. M.; Mohandas, N.; Blackshear, P. L. Measurement of the elastic modulus for red cell membrane using a fluid mechanical technique. *Biophys. J.* **1973**, *13* (8), 747−762.

(30) Edelstein, A.; Amodaj, N.; Hoover, K.; Vale, R.; Stuurman, N. Computer control of microscopes using microManager. *Curr. Protoc. Mol. Biol.* **2010**, *Chapter 14*, 14.20.1−14.20.17.

(31) Schneider, C. A.; Rasband, W. S.; Eliceiri, K. W. NIH Image to ImageJ: 25 years of image analysis. *Nat. Methods* **2012**, *9* (7), 671−5.

(32) Bieling, P.; Laan, L.; Schek, H.; Munteanu, E. L.; Sandblad, L.; Dogterom, M.; Brunner, D.; Surrey, T. Reconstitution of a microtubule plus-end tracking system in vitro. *Nature* **2007**, *450* (7172), 1100−5.

(33) Sarmento, M. J.; Prieto, M.; Fernandes, F. Reorganization of lipid domain distribution in giant unilamellar vesicles upon immobilization with different membrane tethers. *Biochim. Biophys. Acta* **2012**, *1818* (11), 2605−15.

(34) Salentinig, S.; Sagalowicz, L.; Glatter, O. Self-assembled structures and pKa value of oleic acid in systems of biological relevance. *Langmuir* **2010**, *26* (14), 11670−9.

(35) Koster, G.; Cacciuto, A.; Derenyi, I.; Frenkel, D.; Dogterom, M. Force barriers for membrane tube formation. *Phys. Rev. Lett.* **2005**, *94* (6), 068101.

(36) Leduc, C.; Campas, O.; Joanny, J. F.; Prost, J.; Bassereau, P. Mechanism of membrane nanotube formation by molecular motors. *Biochim. Biophys. Acta* **2010**, *1798* (7), 1418−26.

(37) Rossier, O.; Cuvelier, D.; Borghi, N.; Puech, P. H.; Derényi, I.; Buguin, A.; Nassoy, P.; Brochard-Wyart, F. Giant vesicles under flows: Extrusion and retraction of tubes. *Langmuir* **2003**, *19* (3), 575−584.

(38) Waugh, R. E. Surface viscosity measurements from large bilayer vesicle tether formation. II. Experiments. *Biophys. J.* **1982**, *38* (1), 29−37.

(39) Chen, I. A.; Szostak, J. W. Membrane growth can generate a transmembrane pH gradient in fatty acid vesicles. *Proc. Natl. Acad. Sci. U. S. A.* **2004**, *101*, 7965−70.

(40) Bar-Ziv, R.; Moses, E.; Nelson, P. Dynamic excitations in membranes induced by optical tweezers. *Biophys. J.* **1998**, *75* (1), 294−320.

(41) Nelson, P.; Powers, T.; Seifert, U. Dynamical theory of the pearling instability in cylindrical vesicles. *Phys. Rev. Lett.* **1995**, *74* (17), 3384−3387.

(42) Morigaki, K.; Walde, P.; Misran, M.; Robinson, B. H. Thermodynamic and kinetic stability. Properties of micelles and

vesicles formed by the decanoic acid/decanoate system. *Colloids Surf., A* **2003**, *213* (1), 37−44.

(43) Caspi, Y.; Dekker, C. Divided we stand: splitting synthetic cells for their proliferation. *Syst. Synth. Biol.* **2014**, *8* (3), 249−69.

(44) Mercier, R.; Dominguez-Cuevas, P.; Errington, J. Crucial role for membrane fluidity in proliferation of primitive cells. *Cell Rep.* **2012**, *1* (5), 417−23.

(45) Adamala, K.; Szostak, J. W. Nonenzymatic template-directed RNA synthesis inside model protocells. *Science* **2013**, *342* (6162), 1098−100.

(46) Liu, C.; Martin, C. T. Fluorescence characterization of the transcription bubble in elongation complexes of T7 RNA polymerase. *J. Mol. Biol.* **2001**, *308* (3), 465−75.

(47) Ishimaru, M.; Toyota, T.; Takakura, K.; Sugawara, T.; Sugawara, Y. Helical aggregate of oleic acid and its dynamics in water at pH 8. *Chem. Lett.* **2005**, *34* (1), 46−47.